PHYSICAL REVIEW D **92,** 031501(R) (2015)

# High-precision calculation of the strange nucleon electromagnetic form factors

Jeremy Green,[1,*] Stefan Meinel,[2,3,†] Michael Engelhardt,[4] Stefan Krieg,[5,6] Jesse Laeuchli,[7] John Negele,[8] Kostas Orginos,[9,10] Andrew Pochinsky,[8] and Sergey Syritsyn[3]

[1]*Institut für Kernphysik, Johannes Gutenberg-Universität Mainz, D-55099 Mainz, Germany*
[2]*Department of Physics, University of Arizona, Tucson, Arizona 85721, USA*
[3]*RIKEN BNL Research Center, Brookhaven National Laboratory, Upton, New York 11973, USA*
[4]*Department of Physics, New Mexico State University, Las Cruces, New Mexico 88003-8001, USA*
[5]*Bergische Universität Wuppertal, D-42119 Wuppertal, Germany*
[6]*IAS, Jülich Supercomputing Centre, Forschungszentrum Jülich, D-52425 Jülich, Germany*
[7]*Department of Computer Science, College of William and Mary, Williamsburg, Virginia 23187, USA*
[8]*Center for Theoretical Physics, Massachusetts Institute of Technology, Cambridge, Massachusetts 02139, USA*
[9]*Physics Department, College of William and Mary, Williamsburg, Virginia 23187, USA*
[10]*Thomas Jefferson National Accelerator Facility, Newport News, Virginia 23606, USA*

(Received 12 May 2015; published 26 August 2015)

We report a direct lattice QCD calculation of the strange nucleon electromagnetic form factors $G_E^s$ and $G_M^s$ in the kinematic range $0 \leq Q^2 \lesssim 1.2$ GeV$^2$. For the first time, both $G_E^s$ and $G_M^s$ are shown to be nonzero with high significance. This work uses closer to physical lattice parameters than previous calculations, and achieves an unprecedented statistical precision by implementing a recently proposed variance reduction technique called *hierarchical probing*. We perform model-independent fits of the form factor shapes using the $z$-expansion and determine the strange electric and magnetic radii and magnetic moment. We compare our results to parity-violating electron-proton scattering data and to other theoretical studies.

DOI: 10.1103/PhysRevD.92.031501 PACS numbers: 12.38.Gc, 13.40.Em, 13.40.Gp

The nucleon electromagnetic form factors describe how electric charge and current are distributed inside protons and neutrons, and are therefore among the most important observables characterizing these building blocks of ordinary matter. Because nucleons contain only *up* and *down* valence quarks, these two quark flavors dominate the electromagnetic form factors. Isolating the small contributions from the other quark flavors is a significant challenge for both experiment and theory, but is of fundamental importance for our understanding of the structure of protons and neutrons, and of the nonperturbative dynamics of QCD. After the up and down quarks, strange quarks are expected to give the next-largest contribution to the electromagnetic form factors. The cross section of elastic electron-proton scattering used to extract the form factors is dominated by photon exchange, which probes the sum of all quark-flavor contributions weighted according to their electric charges. However, by analyzing the small parity-violating effects arising from interference with $Z$-boson exchange, the strange-quark contribution to the electromagnetic form factors can be isolated [1,2]. The available experimental results, which focus on momentum transfers $Q^2$ in the vicinity of 0.2 GeV$^2$, are consistent with zero but constrain the relative contribution of the strange quarks to be within a few percent [3–15].

*Ab initio* calculations of the nucleon electromagnetic form factors $G_E^q$ and $G_M^q$ of an individual quark flavor $q$ (see, e.g., Ref. [16] for the definitions) are possible using lattice QCD. The form factors can be extracted from Euclidean three-point functions of the form

$$\sum_{\mathbf{z},\mathbf{y}} e^{-i\mathbf{p}'\cdot(\mathbf{z}-\mathbf{y})} e^{-i\mathbf{p}\cdot(\mathbf{y}-\mathbf{x})} \langle N_\beta(z) V_q^\mu(y) \bar{N}_\alpha(x) \rangle, \qquad (1)$$

where $N$ is an interpolating field with the quantum numbers of the nucleon, $V_q^\mu = \bar{q}\gamma^\mu q$ is the vector current for quark flavor $q$, and $\mathbf{p}$, $\mathbf{p}'$ are the spatial momenta of the initial and final states. In the three-point function (1), performing the path integral over the quark fields leaves a path integral over the gauge fields, which contains the product of the fermion determinants and the nonperturbative quark propagator contractions illustrated in Fig. 1. The connected contraction arises only for $q = u, d$ and is numerically large, while the disconnected contraction is present for all quark flavors (and is the origin of the strange-quark contribution to the electromagnetic form factors). The disconnected quark loop in Fig. 1 has the form

$$T_q^\mu = -\sum_{\mathbf{y}} e^{i(\mathbf{p}'-\mathbf{p})\cdot\mathbf{y}} \mathrm{Tr}[\gamma^\mu D_q^{-1}(y,y)], \qquad (2)$$

where $D_q$ is the lattice Dirac operator, and the trace is over color and spin indices. The numerical computation of the propagator $D_q^{-1}(y,y)$ for all spatial lattice points $\mathbf{y}$ using

*green@kph.uni-mainz.de
†smeinel@email.arizona.edu

 

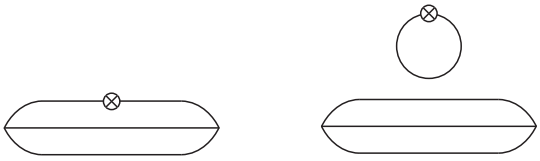

FIG. 1. Nonperturbative quark propagator contractions obtained from Eq. (1) by performing the path integral over the quark fields: connected (left) and disconnected (right).

standard methods is prohibitively expensive for lattices of realistic size, and therefore most lattice calculations of nucleon form factors have been restricted to the connected contractions (and therefore $q = u, d$) only. In Ref. [17], the strange-quark contribution was estimated by combining experimental data for the complete electromagnetic factors with lattice QCD results for the connected $u$- and $d$-quark contractions. This method relies on a delicate cancellation between large quantities, and is therefore limited in its statistical precision and rather susceptible to systematic errors in the lattice calculation.

A direct lattice QCD calculation of the strange-quark contribution can be performed by evaluating the disconnected loop in Eq. (2) stochastically. An unbiased estimate is given by

$$T_q^\mu \approx -\frac{1}{N}\sum_{n=1}^{N}\sum_{\mathbf{y}} e^{i(\mathbf{p}'-\mathbf{p})\cdot\mathbf{y}}\xi_n^\dagger(y)\gamma^\mu\psi_n(y), \tag{3}$$

where $\xi_n$ are suitable noise vectors (for example with random components $\in \mathbb{Z}_2$) with support on the time slice $y_0$, and $\psi_n$ are the corresponding solutions of the lattice Dirac equation, $D_q\psi_n = \xi_n$. Previous unquenched lattice QCD calculations of the strange nucleon electromagnetic form factors using variants of this approach can be found in Refs. [18,19]. The calculation of Ref. [18] was performed on a $16^3 \times 32$ lattice with dimensions $(1.9\text{ fm})^3 \times (3.9\text{ fm})$, and at rather heavy $u$, $d$ quark masses corresponding to pion masses in the range 600–840 MeV. For these parameters, the strange magnetic form factor $G_M^s$ was found to be negative with a significance of $2-3\sigma$ in the region $Q^2 \lesssim 1\text{ GeV}^2$, while the strange electric form factor $G_E^s$ was found to be consistent with zero [18]. The authors of Ref. [19] used an anisotropic $24^3 \times 64$ lattice with dimensions $(2.6\text{ fm})^3 \times (2.3\text{ fm})$ and a pion mass of 416 MeV. The corresponding results for $G_M^s$ and $G_E^s$ have large uncertainties and are consistent with zero.

In this article, we report a new direct lattice QCD calculation of $G_M^s$ and $G_E^s$ with closer-to-physical parameters and with very high statistical precision. For the first time, both $G_M^s$ and $G_E^s$ are shown to be nonzero with high significance and in a wide range of $Q^2$. We also obtain similarly precise results for the analogous disconnected light (equal for up and down) quark contributions, which need to be included in precision lattice calculations of the total electromagnetic form factors of the proton, and are therefore of relevance for the proton charge radius puzzle [20,21]. Our calculation is performed on a large $32^3 \times 96$ lattice of dimensions $(3.6\text{ fm})^3 \times (10.9\text{ fm})$ and includes $2+1$ flavors of dynamical sea quarks, implemented using a clover-improved Wilson action. The up and down quark mass corresponds to a pion mass of 317 MeV, and the strange-quark mass is consistent with the physical value (determined using the "$\eta_s$" mass [22]) within five percent. The unprecedented statistical precision is achieved as follows: (i) we use 1028 gauge-field configurations and compute the three-point function in Eq. (1) for 96 different source locations, $x$, on each configuration, and (ii) we use a novel variance reduction method, hierarchical probing [23], to evaluate the disconnected quark loops $T_q^\mu$. Similarly to *dilution* [24,25], this method is based on the observation that the fluctuations in Eq. (3) due to the random noise vectors originate from the off-diagonal elements of $D_q^{-1}(x,y)$, which decay with the Euclidean distance $|x-y|$. By partitioning the noise vectors into multiple vectors with support only on subsets of the lattice sites, the variance can be reduced (at the cost of additional solutions of the lattice Dirac equation). While dilution is based on a fixed partitioning scheme, hierarchical probing allows one to continuously increase the level of partitioning, eliminating the variance in order of importance while reusing the results from prior levels [23]. This is achieved using a special sequence of Hadamard vectors, $z_n$, which have values $\pm 1$ on the lattice sites. Examples of $z_n$ are shown in Fig. 2. In Eq. (3), we make the replacement

$$\xi_n \to z_n \odot \xi, \tag{4}$$

where $\xi$ is a single noise vector and $\odot$ denotes the element-wise Hadamard product [23]. As mentioned earlier, we use noise vectors with support only on selected time slices, and we therefore perform three-dimensional hierarchical probing. We use $N = 128$ Hadamard vectors, which eliminates the variance from neighboring lattice sites up to distance 4. For the electromagnetic form factors, we observe a variance

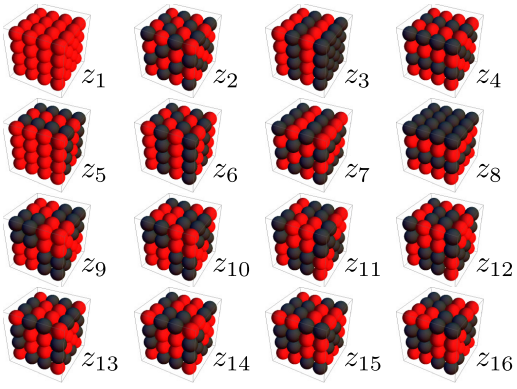


FIG. 2 (color online). The first 16 Hadamard vectors for hierarchical probing on a $4^3$ lattice; red $= +1$, black $= -1$.

reduction by approximately a factor of 10 compared to the traditional noise method with the same $N$ (at equal computational cost). Our calculation employs complex $\mathbb{Z}_2 \times \mathbb{Z}_2$ noise and also uses color and spin dilution for the noise vectors $\xi$.

We use the lattice conserved vector current [generalizing Eqs. (2)–(3) for currents that are not site local] including an improvement term [26,27] to reduce $O(a)$ lattice artifacts, where $a$ is the lattice spacing, with the improvement coefficient set to its tree-level value. We independently vary the momenta $\mathbf{p}$ and $\mathbf{p}'$ to obtain 59 different values of $Q^2$. For clarity in plots we bin the nearest points that have the same $(\mathbf{p}' - \mathbf{p})^2$ and $|\mathbf{p}'^2 - \mathbf{p}^2|$, and thus differ in $Q^2$ by less than 0.006 GeV$^2$. The three-point function (1) receives contributions from the desired nucleon ground state and from excited states; the excited-state contributions decay exponentially faster with the source-sink separation, $|z_0 - x_0|$, than the ground-state contribution. We use $|z_0 - x_0| \approx 1.14$ fm for our main results, and estimate the remaining excited-state contamination using a second separation of $|z_0 - x_0| \approx 1.37$ fm.

Our calculated form factors are shown in Fig. 3. $G_E^s(Q^2)$ is consistent with zero at $Q^2 = 0$ and positive for all other values of $Q^2$. It rises with $Q^2$ until it reaches a maximum value around 0.003, somewhere between 0.2 and 1.0 GeV$^2$, above which the data hint at a decrease. In the same range, $G_M^s(Q^2)$ is negative, with a decrease in magnitude with $Q^2$ up to around 0.5 GeV$^2$. Above that, the data are consistent with a constant. Note that data with the same spatial momentum transfer $\mathbf{q} = \mathbf{p} - \mathbf{p}'$ tend to have strongly correlated errors, meaning that, e.g., the points below $Q^2 = 0.4$ GeV$^2$ form three clusters of correlated data that should not be interpreted as "bumpy" behavior in the form factor. The disconnected light-quark form factors have similar dependence on $Q^2$ but their magnitude is two to three times that of the strange-quark form factors.

We fit the $Q^2$-dependence of each form factor using the $z$-expansion [28,29],

$$G(Q^2) = \sum_k^{k_{\max}} a_k z^k, \quad z = \frac{\sqrt{t_{\rm cut} + Q^2} - \sqrt{t_{\rm cut}}}{\sqrt{t_{\rm cut} + Q^2} + \sqrt{t_{\rm cut}}}, \tag{5}$$

which conformally maps the complex domain of analyticity in $Q^2$ to $|z| < 1$. Although for physical quark masses the isoscalar threshold is $t_{\rm cut} = (3m_\pi)^2$, at our pion mass we expect that the $\omega$ resonance is a stable particle below threshold; therefore, we use the isovector threshold $t_{\rm cut} = (2m_\pi)^2$ in our fits. The intercept and slope of the form factor at $Q^2 = 0$ can be obtained from the first two coefficients, $a_0$ (which we fix to zero for $G_E$) and $a_1$. We impose Gaussian priors on the remaining coefficients, centered at zero with width equal to 5 $\max\{|a_0|, |a_1|\}$. We truncate the series with $k_{\max} = 5$, but we have verified that using $k_{\max} = 10$ produces identical fit results in our probed range of $Q^2$. The resulting fit curves are shown in Fig. 3.

The uncertainties are estimated as follows:

(1) Statistical uncertainties are computed using jackknife resampling, using samples binned from four gauge configurations. These are shown as the inner error bands in Fig. 3.

(2) Fitting uncertainties are estimated by doubling and halving the widths of the fit priors, as well as performing the fits using different estimations of correlations in the data.

(3) For the light-quark disconnected form factors, we estimate excited-state errors by computing the form factors using a larger source-sink separation, 1.37 fm. We assign the same relative error due to excited states to the strange-quark form factors.

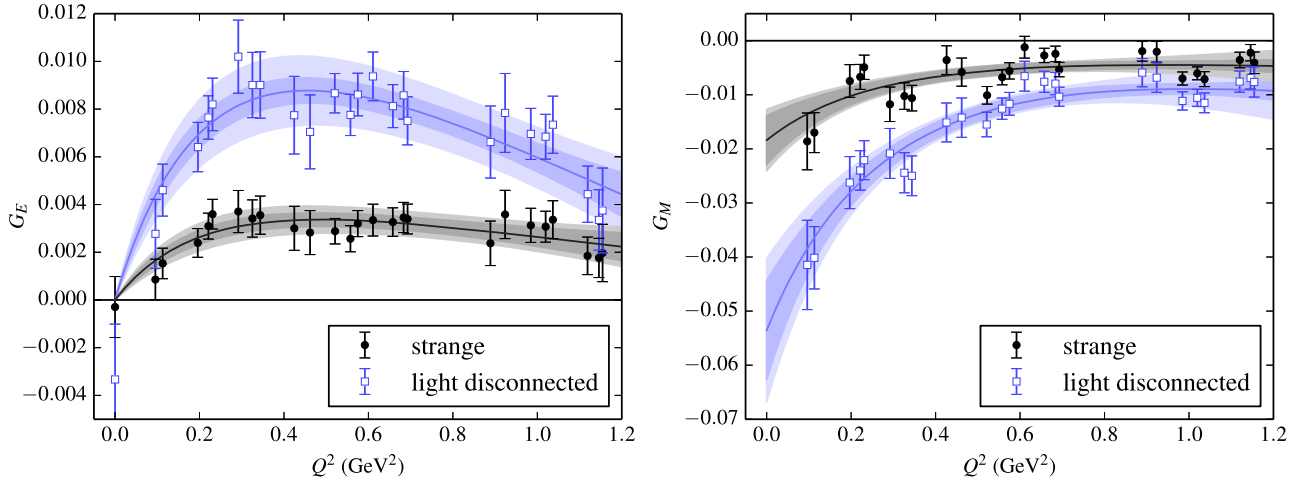


FIG. 3 (color online). Strange-quark and disconnected light-quark electric and magnetic form factors, with statistical error bars. The curves result from the $z$-expansion fits; the inner bands show the statistical uncertainty and the outer error bands show the combined statistical and systematic uncertainties (added in quadrature). The charge factors are not included.

(4) Uncertainties due to discretization effects are estimated by comparing against the form factors computed using the unimproved current.

The outer error bands in Fig. 3 show the sum of these uncertainties in quadrature. We neglect finite-volume effects since they are highly suppressed by $e^{-m_\pi L}$, with $m_\pi L = 5.9$. Our resulting strange radii $(r^2_{E,M})^s \equiv -6\mathrm{d}G^s_{E,M}/\mathrm{d}Q^2|_{Q^2=0}$ and strange magnetic moment $\mu^s \equiv G^s_M(0)\mu^{\mathrm{lat}}_N$ at pion mass 317 MeV are the following:

$$\begin{aligned}(r^2_E)^s &= -0.0054(9)(6)(11)(2)\ \mathrm{fm}^2,\\ (r^2_M)^s &= -0.0147(61)(28)(34)(5)\ \mathrm{fm}^2,\\ \mu^s &= -0.0184(45)(12)(32)(1)\mu^{\mathrm{lat}}_N,\end{aligned} \tag{6}$$

where the four uncertainties are given in the same order as listed above, and $\mu^{\mathrm{lat}}_N$ is the nuclear magneton using the lattice nucleon mass, 1067(8) MeV. We find that the leading sources of uncertainty are statistics, as expected for disconnected diagrams, and excited-state effects, which have been found to be important for many nucleon observables (see, e.g., [16,30–33]). Our estimate of discretization effects is negligible by comparison, which is consistent with calculations of other nucleon observables that used multiple lattice spacings to probe the continuum limit (see, e.g., [30,32–39]).

Although a controlled extrapolation to the physical point would require several lattice ensembles with varying quark masses, an estimate can be made by combining strange-quark data with the equivalent obtained from the disconnected light-quark form factors. By itself, the latter can be understood in the framework of partially quenched QCD [40,41] by introducing a third light-quark flavor (which couples to the current in the quark-disconnected loop) and a bosonic ghost quark (which cancels all other loops). The dependence of the strange radii and magnetic moment on quark masses has been studied in SU(3) heavy-baryon chiral perturbation theory (ChPT) [42–44], and its partially quenched generalization [45–47]. At leading one-loop order, these observables depend only on the mass $m_{\mathrm{loop}}$ of a pseudoscalar meson composed of a nucleon valence quark and a quark from the vector current. For strange-quark and disconnected light-quark observables, $m_{\mathrm{loop}}$ is $m_K$ and $m_\pi$, respectively, and we can interpolate to the physical kaon mass. However, using typical values of the meson decay constant and meson-baryon couplings from phenomenology predicts a much stronger dependence on $m_{\mathrm{loop}}$ than we observe, suggesting that the quark masses are too large for ChPT at this order. Therefore, we resort to a simple linear interpolation in $m^2_{\mathrm{loop}}$. We also adjust to the physical nuclear magneton, and obtain the following estimates at the physical point:

$$\begin{aligned}(r^2_E)^s &= -0.0067(10)(17)(15)\ \mathrm{fm}^2,\\ (r^2_M)^s &= -0.018(6)(5)(5)\ \mathrm{fm}^2,\\ \mu^s &= -0.022(4)(4)(6)\mu_N,\end{aligned} \tag{7}$$

where the first two uncertainties are statistical and systematic (as estimated above). The third error is the difference between the value at the physical point and our lattice ensemble (using the physical nuclear magneton), and serves as an estimate of the uncertainty due to extrapolation to the physical point. As a cross-check, we also performed extrapolations including only our strange-quark data at $m_\pi = 317$ MeV and the strange-quark data at $m_\pi = 600$ MeV from Ref. [18]. The results are consistent with Eq. (7) within the given extrapolation uncertainties.

The experiments run at forward scattering angles were sensitive to a particular linear combination of form factors, $G^s_E + \eta G^s_M$, which we show in Fig. 4. Our results and the experimental data are both broadly consistent with zero, although the lattice data have much smaller uncertainties. This suggests that it will be quite challenging for future experiments to obtain a clear nonzero strange-quark signal at forward angles.

Figure 5 shows a comparison with some other determinations of the strange magnetic moment. The value from experiment has the largest uncertainty and is consistent with the other shown results. This work is in agreement with the other values within $2\sigma$, except for two of the dispersion-theory scenarios [48], and has the smallest uncertainty.

The techniques used in this work have proven effective in dealing with the longstanding problem of noise in disconnected contributions to matrix elements. Although

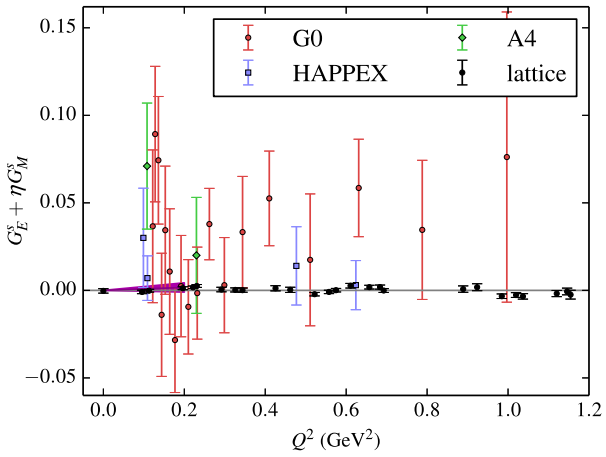


FIG. 4 (color online). Linear combination of form factors, $G^s_E + \eta G^s_M$, probed by forward-angle parity-violating elastic $ep$ scattering experiments [6–8,10–12,14,15]. The coefficient $\eta$ depends on the scattering angle and $Q^2$; for the lattice data we use the approximation $\eta = AQ^2$, $A = 0.94$ GeV$^{-2}$ [11]. In the low $Q^2$ region we also show the linear dependence on $Q^2$ resulting from the estimated charge radius and magnetic moment at the physical point.

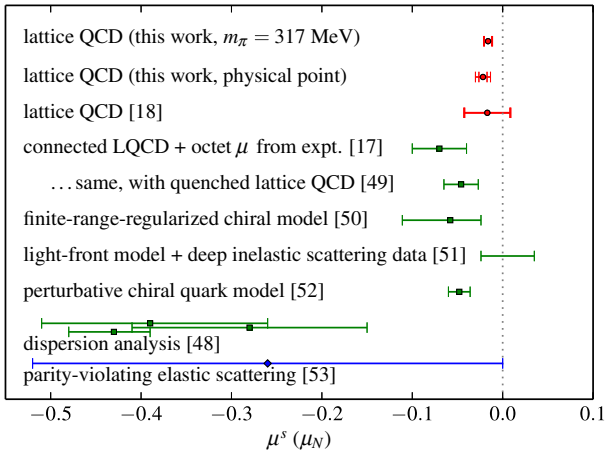


FIG. 5 (color online). Determinations of the strange magnetic moment: from direct lattice QCD calculations (this work and Ref. [18]; red circles), models and phenomenology [17,48–52] (green squares), and from a recent global analysis of parity-violating elastic scattering data [53] (blue diamond).

future calculations at near-physical quark masses will be needed to confirm our physical-point estimates, we have found very small contributions from strange quarks to proton electromagnetic observables: including the charge factor of $-1/3$ yields a roughly 0.3% effect in the proton $r_E^2$, $\mu r_M^2$, and $\mu$.

## ACKNOWLEDGMENTS

Computations for this work were carried out on facilities of the USQCD Collaboration, which are funded by the Office of Science of the U.S. Department of Energy (DOE), and on facilities provided by XSEDE, funded by the National Science Foundation Grant No. ACI-1053575. During this research J. G., S. M., J. N., and A. P. were supported in part by the U.S. Department of Energy Office of Nuclear Physics under Award No. DE–FG02–94ER40818; M. E. was supported in part by DOE Award No. DE–FG02–96ER40965; J. L. was supported in part by DOE Award No. DE–FC02–12ER41890 and NSF Grant No. CCF-121834; K. O. was supported in part by DOE Award No. DE-FG02-04ER41302 and also DOE Award No. DE-AC05-06OR23177, under which JSA operates the Thomas Jefferson National Accelerator Facility; S. S. was supported in part by DOE Award No. DE–AC02–05CH11231 and the RIKEN Foreign Postdoctoral Researcher Program; and S. K. was supported in part by Deutsche Forschungsgemeinschaft through Grant No. SFB–TRR 55. J. G. was also supported in part by the PRISMA Cluster of Excellence at the University of Mainz, and S. M. was also supported in part by the RHIC Physics Fellow Program of the RIKEN BNL Research Center. Calculations were performed with the Chroma software suite [54], using QUDA [55] with multi-GPU support [56].

[1] D. B. Kaplan and A. Manohar, Strange matrix elements in the proton from neutral current experiments, Nucl. Phys. **B310**, 527 (1988).
[2] R. McKeown, Sensitivity of polarized elastic electron proton scattering to the anomalous baryon number magnetic moment, Phys. Lett. B **219**, 140 (1989).
[3] R. Hasty *et al.* (SAMPLE Collaboration), Strange magnetism and the anapole structure of the proton, Science **290**, 2117 (2000).
[4] D. Spayde *et al.* (SAMPLE Collaboration), The strange quark contribution to the proton's magnetic moment, Phys. Lett. B **583**, 79 (2004).
[5] E. Beise, M. Pitt, and D. Spayde, The SAMPLE experiment and weak nucleon structure, Prog. Part. Nucl. Phys. **54**, 289 (2005).
[6] K. Aniol *et al.* (HAPPEX Collaboration), Parity-violating electroweak asymmetry in polarized $\vec{e}p$ scattering, Phys. Rev. C **69**, 065501 (2004).
[7] F. Maas *et al.* (A4 Collaboration), Measurement of Strange Quark Contributions to the Nucleon's Form Factors at $Q^2 = 0.230$ $(\mathrm{GeV}/c)^2$, Phys. Rev. Lett. **93**, 022002 (2004).
[8] F. Maas, K. Aulenbacher, S. Baunack, L. Capozza, J. Diefenbach *et al.*, Evidence for Strange Quark Contributions to the Nucleon's Form Factors at $Q^2 = 0.108$ $(\mathrm{GeV}/c)^2$, Phys. Rev. Lett. **94**, 152001 (2005).
[9] K. Aniol *et al.* (HAPPEX Collaboration), Parity-Violating Electron Scattering from $^4$He and the Strange Electric Form Factor of the Nucleon, Phys. Rev. Lett. **96**, 022003 (2006).
[10] K. Aniol *et al.* (HAPPEX Collaboration), Constraints on the nucleon strange form factors at $Q^2 \sim 0.1$ GeV$^2$, Phys. Lett. B **635**, 275 (2006).
[11] D. Armstrong *et al.* (G0 Collaboration), Strange Quark Contributions to Parity-Violating Asymmetries in the Forward G0 Electron-Proton Scattering Experiment, Phys. Rev. Lett. **95**, 092001 (2005).
[12] A. Acha *et al.* (HAPPEX Collaboration), Precision Measurements of the Nucleon Strange Form Factors at $Q^2 \sim 0.1$ GeV$^2$, Phys. Rev. Lett. **98**, 032301 (2007).
[13] D. Androic *et al.* (G0 Collaboration), Strange Quark Contributions to Parity-Violating Asymmetries in the Backward Angle G0 Electron Scattering Experiment, Phys. Rev. Lett. **104**, 012001 (2010).
[14] S. Baunack, K. Aulenbacher, D. Balaguer Rios, L. Capozza, J. Diefenbach *et al.*, Measurement of Strange Quark Contributions to the Vector Form Factors of the Proton at $Q^2 = 0.22$ $(\mathrm{GeV}/c)^2$, Phys. Rev. Lett. **102**, 151803 (2009).

[15] Z. Ahmed *et al.* (HAPPEX Collaboration), New Precision Limit on the Strange Vector Form Factors of the Proton, Phys. Rev. Lett. **108**, 102001 (2012).

[16] J. R. Green, J. W. Negele, A. V. Pochinsky, S. N. Syritsyn, M. Engelhardt, and S. Krieg, Nucleon electromagnetic form factors from lattice QCD using a nearly physical pion mass, Phys. Rev. D **90**, 074507 (2014).

[17] P. E. Shanahan, R. Horsley, Y. Nakamura, D. Pleiter, P. E. L. Rakow, G. Schierholz, H. Stüben, A. W. Thomas, R. D. Young, and J. M. Zanotti, Determination of the Strange Nucleon Form Factors, Phys. Rev. Lett. **114**, 091802 (2015).

[18] T. Doi, M. Deka, S.-J. Dong, T. Draper, Keh-Fei Liu, D. Mankame, N. Mathur, and T. Streuer, Nucleon strangeness form factors from $N_f = 2 + 1$ clover fermion lattice QCD, Phys. Rev. D **80**, 094503 (2009).

[19] R. Babich, R. C. Brower, M. A. Clark, G. T. Fleming, J. C. Osborn, C. Rebbi, and D. Schaich, Exploring strange nucleon form factors on the lattice, Phys. Rev. D **85**, 054510 (2012).

[20] R. Pohl, A. Antognini, F. Nez, F. D. Amaro, F. Biraben *et al.*, The size of the proton, Nature (London) **466**, 213 (2010).

[21] A. Antognini, F. Nez, K. Schuhmann, F. D. Amaro, F. Biraben *et al.*, Proton structure from the measurement of $2S - 2P$ transition frequencies of muonic hydrogen, Science **339**, 417 (2013).

[22] R. Dowdall *et al.* (HPQCD Collaboration), The Upsilon spectrum and the determination of the lattice spacing from lattice QCD including charm quarks in the sea, Phys. Rev. D **85**, 054509 (2012).

[23] A. Stathopoulos, J. Laeuchli, and K. Orginos, Hierarchical probing for estimating the trace of the matrix inverse on toroidal lattices, SIAM J. Sci. Comput. **35**, S299 (2013).

[24] W. Wilcox, *Numerical Challenges in Lattice Quantum Chromodynamics*, edited by A. Frommer, T. Lippert, B. Medeke, and K. Schilling, Lecture Notes in Computational Science and Engineering, Vol. 15 (Springer, Berlin Heidelberg, 2000), p. 127.

[25] J. Foley, K. Jimmy Juge, A. Ó. Cais, M. Peardon, S. M. Ryan, and Jon-Ivar Skullerud, Practical all-to-all propagators for lattice QCD, Comput. Phys. Commun. **172**, 145 (2005).

[26] G. Martinelli, C. T. Sachrajda, and A. Vladikas, A study of "improvement" in lattice QCD, Nucl. Phys. **B358**, 212 (1991).

[27] S. Boinepalli, D. Leinweber, A. Williams, J. Zanotti, and J. Zhang, Precision electromagnetic structure of octet baryons in the chiral regime, Phys. Rev. D **74**, 093005 (2006).

[28] R. J. Hill and G. Paz, Model-independent extraction of the proton charge radius from electron scattering, Phys. Rev. D **82**, 113005 (2010).

[29] Z. Epstein, G. Paz, and J. Roy, Model-independent extraction of the proton magnetic radius from electron scattering, Phys. Rev. D **90**, 074027 (2014).

[30] S. Capitani, M. Della Morte, G. von Hippel, B. Jäger, A. Jüttner, B. Knippschild, H. B. Meyer, and H. Wittig, The nucleon axial charge from lattice QCD with controlled errors, Phys. Rev. D **86**, 074502 (2012).

[31] J. R. Green, M. Engelhardt, S. Krieg, J. W. Negele, A. V. Pochinsky, and S. N. Syritsyn, Nucleon structure from lattice QCD using a nearly physical pion mass, Phys. Lett. B **734**, 290 (2014).

[32] G. S. Bali, S. Collins, B. Gläßle, M. Göckeler, J. Najjar, R. H. Rödl, A. Schäfer, R. W. Schiel, W. Söldner, and A. Sternbeck, Nucleon isovector couplings from $N_f = 2$ lattice QCD, Phys. Rev. D **91**, 054501 (2015).

[33] M. Constantinou, Hadron structure, *Proc. Sci.*, LATTICE2014 (2015) 001.

[34] J. R. Green, J. W. Negele, A. V. Pochinsky, S. N. Syritsyn, M. Engelhardt, and S. Krieg, Nucleon scalar and tensor charges from lattice QCD with light Wilson quarks, Phys. Rev. D **86**, 114509 (2012).

[35] C. Alexandrou, M. Constantinou, S. Dinter, V. Drach, K. Hadjiyiannakou, K. Jansen, G. Koutsou, and A. Vaquero, Strangeness of the nucleon from lattice QCD, Phys. Rev. D **91**, 094503 (2015).

[36] C. Alexandrou, M. Brinet, J. Carbonell, M. Constantinou, P. A. Harraud, P. Guichon, K. Jansen, T. Korzec, and M. Papinutto, Nucleon electromagnetic form factors in twisted mass lattice QCD, Phys. Rev. D **83**, 094502 (2011).

[37] S. Collins, M. Göckeler, P. Hägler, R. Horsley, Y. Nakamura *et al.*, Dirac and Pauli form factors from lattice QCD, Phys. Rev. D **84**, 074507 (2011).

[38] S. Syritsyn, J. Bratt, M. Lin, H. Meyer, J. Negele *et al.*, Nucleon electromagnetic form factors from lattice QCD using $2 + 1$ flavor domain wall fermions on fine lattices and chiral perturbation theory, Phys. Rev. D **81**, 034507 (2010).

[39] T. Bhattacharya, V. Cirigliano, S. Cohen, R. Gupta, A. Joseph *et al.*, Isovector and isoscalar tensor charges of the nucleon from lattice QCD, arXiv:1506.06411.

[40] C. W. Bernard and M. F. Golterman, Partially quenched gauge theories and an application to staggered fermions, Phys. Rev. D **49**, 486 (1994).

[41] M. Della Morte and A. Jüttner, Quark disconnected diagrams in chiral perturbation theory, J. High Energy Phys. 11 (2010) 154.

[42] M. Musolf and H. Ito, Chiral symmetry and the nucleon's vector strangeness form factors, Phys. Rev. C **55**, 3066 (1997).

[43] T. R. Hemmert, U.-G. Meissner, and S. Steininger, Strange magnetism in the nucleon, Phys. Lett. B **437**, 184 (1998).

[44] T. R. Hemmert, B. Kubis, and U.-G. Meissner, Strange chiral nucleon form factors, Phys. Rev. C **60**, 045501 (1999).

[45] J.-W. Chen and M. J. Savage, Baryons in partially quenched chiral perturbation theory, Phys. Rev. D **65**, 094001 (2002).

[46] D. Arndt and B. C. Tiburzi, Charge radii of the meson and baryon octets in quenched and partially quenched chiral perturbation theory, Phys. Rev. D **68**, 094501 (2003).

[47] D. B. Leinweber, Quark contributions to baryon magnetic moments in full, quenched and partially quenched QCD, Phys. Rev. D **69**, 014005 (2004).

[48] H. Hammer and M. Ramsey-Musolf, $K\bar{K}$ continuum and isoscalar nucleon form factors, Phys. Rev. C **60**, 045204 (1999).

[49] D. B. Leinweber, S. Boinepalli, I. C. Cloet, A. W. Thomas, A. G. Williams, R. D. Young, J. M. Zanotti, and J. B. Zhang, Precise Determination of the Strangeness Magnetic Moment of the Nucleon, Phys. Rev. Lett. **94**, 212001 (2005).

[50] P. Wang, D. Leinweber, and A. Thomas, Strange magnetic form factor of the nucleon in a chiral effective model at next-to-leading order, Phys. Rev. D **89**, 033008 (2014).

[51] T. Hobbs, M. Alberg, and G. A. Miller, Constraining nucleon strangeness, Phys. Rev. C **91**, 035205 (2015).

[52] V. E. Lyubovitskij, P. Wang, T. Gutsche, and A. Faessler, Strange nucleon form factors in the perturbative chiral quark model, Phys. Rev. C **66**, 055204 (2002).

[53] R. González-Jiménez, J. Caballero, and T. Donnelly, Global analysis of parity-violating asymmetry data for elastic electron scattering, Phys. Rev. D **90**, 033002 (2014).

[54] R. G. Edwards and B. Joó (SciDAC, LHPC, UKQCD Collaboration), The Chroma software system for lattice QCD, Nucl. Phys. B, Proc. Suppl. **140**, 832 (2005).

[55] M. Clark, R. Babich, K. Barros, R. Brower, and C. Rebbi, Solving lattice QCD systems of equations using mixed precision solvers on GPUs, Comput. Phys. Commun. **181**, 1517 (2010).

[56] R. Babich, M. A. Clark, B. Joó, G. Shi, R. C. Brower, and S. Gottlieb, Scaling lattice QCD beyond 100 GPUs, in *Proceedings of 2011 International Conference for High Performance Computing, Networking, Storage and Analysis* (ACM, New York, 2011), p. 70.